

Lighting Condition Analysis for Mars' Moon Phobos

Zu Qun Li
NASA Johnson Space Center
2101 NASA Road 1
Houston, TX 77058
zuqun.li@nasa.gov

Guy de Carufel
Odyssey Space Research llc
NASA Johnson Space Center
Houston, TX 77058
guy.decarufel@nasa.gov

Edwin Z. Crues
NASA Johnson Space Center
2101 NASA Road 1
Houston, TX 77058
edwin.z.crues@nasa.gov

Paul Bielski
NASA Johnson Space Center
2101 NASA Road 1
Houston, TX 77058
paul.bielski@nasa.gov

Abstract—This study used high fidelity computer simulation to investigate the lighting conditions, specifically the solar radiation flux over the surface, on Phobos. Ephemeris data from the Jet Propulsion Laboratory (JPL) DE405 model was used to model the state of the Sun, Earth, Moon, and Mars. An occultation model was developed to simulate Phobos' self-shadowing and its solar eclipses by Mars. The propagated Phobos state was compared with data from JPL's Horizon system to ensure the accuracy of the result. Results for Phobos lighting conditions over one Martian year are presented, which include the duration of solar eclipses, average solar radiation intensity, surface exposure time, and radiant exposure for both sun tracking and fixed solar arrays. The results show that: Phobos' solar eclipse time varies throughout the Martian year, with longer eclipse durations during the Martian northern spring and fall seasons and no eclipses during the Martian northern summer and winter seasons; solar radiation intensity is close to minimum in late spring and close to maximum in late fall; exposure time per orbit is relatively constant over the surface during the spring and fall but varies with latitude during the summer and winter; and Sun tracking solar arrays generate more energy than a fixed solar array. A usage example of the result is also present in this paper to demonstrate the utility.

tionally, tele-operating Mars surface robots from Phobos will incur significantly lower communication delays compared to tele-operating from Earth. This near real time commanding could allow an in-depth study of Mars and potentially allow robotic constructions to prepare for a later human arrival [2], [4]. Besides the technical benefits, a human mission to Phobos will stimulate public interest in space exploration, inspiring the next generation of scientists, engineers, and space explorers [2], [3], [4].

To ensure the success of a Phobos mission, a comprehensive understanding of Phobos' environment is required. Solar radiation plays a crucial role in power and thermal subsystems for a solar-powered vehicle. A thorough understanding of solar radiation on Phobos allows engineers to appropriately size the solar arrays and the batteries for the power subsystem. It also provides important information for astronauts to choose the optimal path of the mobility vehicle. This paper focuses on the power subsystem as an example to demonstrate the usage of Phobos lighting condition data.

This study uses high fidelity computer simulation to investigate the lighting conditions, specifically solar radiation, on the Phobos surface over one Martian year. The computer simulation was developed using Johnson Space Center's (JSC) in-house simulation tools in order to: (a) model the states of the Sun, Earth, Mars, and the Moon using JPL DE405 model; (b) model the orbit of Phobos, its surface, and its gravitational field; (c) model the occultation of Phobos' surface due to solar eclipse by Mars and self-shadowing.

The result of the analysis contains average radiation intensity on Phobos and surface radiation flux. This data allows us to determine surface exposure time based on Phobos orbit, duration of solar eclipse by Mars, radiation flux for a fixed solar array, and radiation flux for a perfectly sun-tracking solar array. The data showed that the lighting condition on Phobos' surface changes dramatically from one Martian season to another. This presents a challenge in the vehicle design for a long duration mission on Phobos.

The remainder of this paper is organized as follows. Section 2 describes development of the high fidelity computer simulation. Section 3 presents the lighting condition analysis result of Phobos for one Martian year. Section 4 shows the utility of the lighting condition data. Section 5 enumerates the conclusions of this study.

TABLE OF CONTENTS

1. INTRODUCTION.....	1
2. SIMULATION DEVELOPMENT	2
3. ANALYSIS RESULTS	2
4. USAGE EXAMPLE.....	5
5. CONCLUSION	5
APPENDIX	5
ACKNOWLEDGMENTS	9
REFERENCES	9
BIOGRAPHY	9

1. INTRODUCTION

Many studies have suggested that a human mission to Phobos is an important precursor and catalyst for NASA's human missions to Mars [1], [2], [3], [4]. Since Phobos does not have an atmosphere, the mission does not require a complex aerocapture system for surface exploration. Moreover, a mission to Phobos can be achieved with smaller minimum ΔV than a mission to Mars [2], [3]. Many technologies developed for a human Phobos mission are fundamental elements for a successful human Mars mission[3], [4]. Addi-

2. SIMULATION DEVELOPMENT

A high fidelity model was developed using JSC in-house simulation tools to generate the data needed for the analysis. The simulation contains three major components including an environment model, a Phobos model, and an occultation model. These three components are inter-connected to produce the presented results. Figure 1 illustrates an overview of the simulation structure.

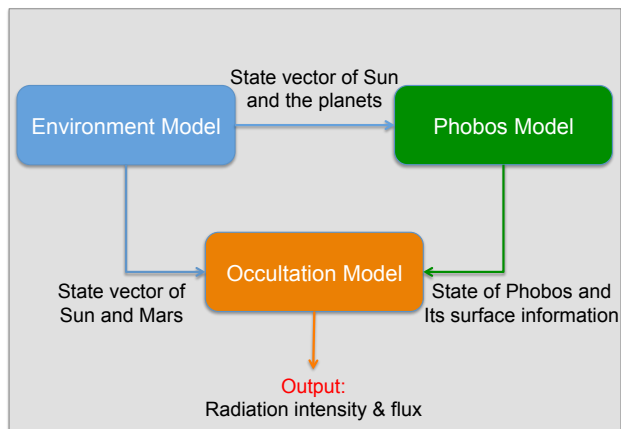


Figure 1. Phobos lighting simulation structure.

Environment Model

The environment model, developed using JSC Engineering Orbital Dynamic (JEOD) package, contains models of the Sun, Earth, Moon, and Mars. The state data of these planets and the Sun were generated using JPL ephemeris file DE405, which contains highly accurate ephemeris data of major bodies in our solar system[5]. A spherical gravitational model was used for the Sun, Earth, and Moon. A 10-degree spherical harmonic gravitational model was used for Mars. JEOD manages the state of all bodies, including Phobos, using a tree-structured reference frame system that calculates an accurate gravitational acceleration for Phobos' state propagation. Deimos was not included in the simulation due to its negligible gravitational effect.

Phobos Model

The Phobos model contains a dynamics model, a surface model, and a gravitational model. The dynamics model was managed by JEOD for state propagation to obtain an accurate state of Phobos with respect to other bodies. The surface model simulates the detailed shape of Phobos, which was used in the gravitational and the occultation models. A polyhedron gravitational representation technique is used to determine the gravitational field of Phobos. Figure 2 illustrates one of the STL models of Phobos used in the study.

Occultation Model

This study used an occultation model that determines if any STL facet is being shadowed by any other facet representing the surface of Phobos. The occultation model uses a point to point ray-trace from the subject facet to a point source, in this case the Sun. The model then solves for any intersection of this ray-trace by all other facets, which results in the subject facet being shadowed if it is intersected. An optimization routine groups multiple facets into spherical coordinate height fields so that only facets of relevant height fields are considered during the occultation determination.



Figure 2. Phobos STL model used in the study.

3. ANALYSIS RESULTS

The lighting condition of Phobos' surface from July 05, 2030 to May 22, 2032 was generated using the simulation developed for the study. The time span covers all four Martian seasons, and Table 1 shows equinoxes and solstices of Mars using the northern hemisphere as a reference[6]. In Table 1, L_s represents solar longitude since vernal equinox (beginning of northern spring).

The propagated state of Phobos was validated with data from JPL Horizon system, and Figure 3 shows the position and velocity error of the propagated Phobos state. The average position error is $26.7m$ with a standard deviation of $21.6m$. The average velocity error is $0.006044m/s$ with a standard deviation of $0.0044m/s$.

Figure 4 shows the instantaneous lighting condition of Phobos on April 01, 2030 00:00:00 using a 5040 facet STL model. This date is between a Martian northern winter and spring such that the solar flux is higher in the southern hemisphere. The geological map of Phobos used in Figure 4, and later in Figure 6 through Figure 8 was obtained from the U.S. Geological Survey (USGS)[7].

The following subsections present post-processed results using the lighting conditions data. The equations used for computing the results are presented in the Appendix.

Average Radiation Intensity and Solar Eclipse

Figure 5 shows the average radiation intensity on Phobos and solar eclipse time per orbit over one Martian year.

The variation in solar radiation intensity on Phobos is due to its distance from the Sun. The minimum intensity occurs in late northern spring as Mars is at aphelion, whereas the maximum intensity occurs in late fall as Mars is at perihelion. Due to the inclination angle of Phobos' orbit with respect to Mars' orbital plane, the eclipse time ranges from 55 minutes at the spring and fall equinoxes to zero minutes at the summer and winter solstices.

Table 1. Martian season (northern hemisphere perspective)

Year	Spring Equinox $L_s = 0^\circ$	Summer Solstice $L_s = 90^\circ$	Fall Equinox $L_s = 180^\circ$	Winter Solstice $L_s = 270^\circ$
1	Apr 11, 1955	Oct 27, 1955	Apr 27, 1956	Sep 21, 1956
⋮	⋮	⋮	⋮	⋮
39	Sep 30, 2026	Apr 16, 2027	Oct 17, 2027	Mar 12, 2028
40	Aug 17, 2028	Mar 03, 2029	Sep 03, 2029	Jan 28, 2030
41*	Jul 05, 2030	Jan 19, 2031	Jul 22, 2031	Dec 16, 2031
42*	May 22, 2032	dec 06, 2032	Jun 08, 2033	Nov 02, 2033
*	estimates based on the orbital period of Mars			

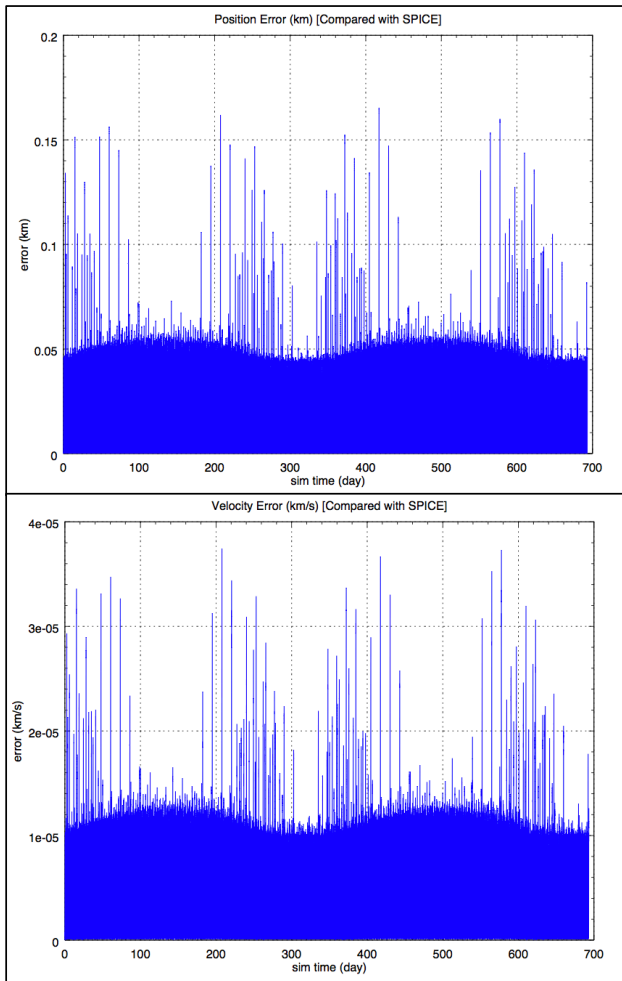


Figure 3. Propagated state error of Phobos

Surface Exposure Time per Orbit

Using the lighting conditions data, the sunlight exposure time of Phobos’ surface per orbital period was determined. The results show that: (a) exposure time is relatively uniform over the surface at northern spring equinox with a shorter exposure at the sub-Mars area (surface facing Mars) and a longer exposure at the anti-Mars area; (b) moving towards the summer solstice, exposure decreases in the southern hemisphere and increases in the northern hemisphere, reaching a maximum variance at the summer solstice; (c) exposure time becomes

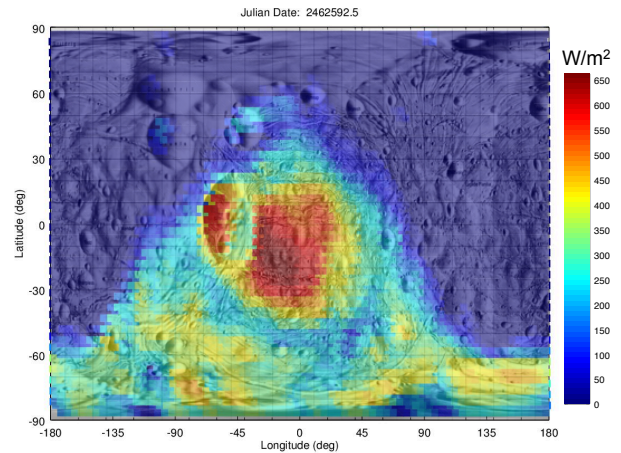


Figure 4. Lighting condition on April 01, 2030 00:00:00

relatively uniform again as time progresses from summer to fall; (d) then finally, exposure increases in the southern hemisphere and decreases in the northern hemisphere as time progresses towards the winter solstice. Figure 6 shows four instances of the surface exposure time per Phobos orbit at the equinoxes and solstices. This information may prove useful in determining the sizing requirement of the power subsystem of a lander such that it may operate for extended periods, including periods of shadowing.

Radiation Energy per Orbit

The radiation energy results contain two parts: (a) the radiant exposure (energy per unit area) for a fixed solar array; (b) the radiant exposure for a perfectly sun tracking array. Based on these results, a sun tracking solar array could generate 50 to 75 percent more energy than a fixed solar array, depending on the time of the Martian year and the location on Phobos. Both cases measure the amount of solar energy per unit area that is accumulated for one Phobos orbit as a function of time.

Radiant Exposure for Fixed Solar Array—represents a conservative scenario for energy generation. It assumed the solar array is orientated parallel to the surface of Phobos without tracking the motion of the sun. The results account for effects of solar radiation intensity, exposure time, and incident angle of the sun light. Similar to the exposure time, the radiant exposure changes from one season to another. Figure 7 shows four instances of the fixed array radiant exposure over one Phobos orbit around Mars at equinoxes and solstices.

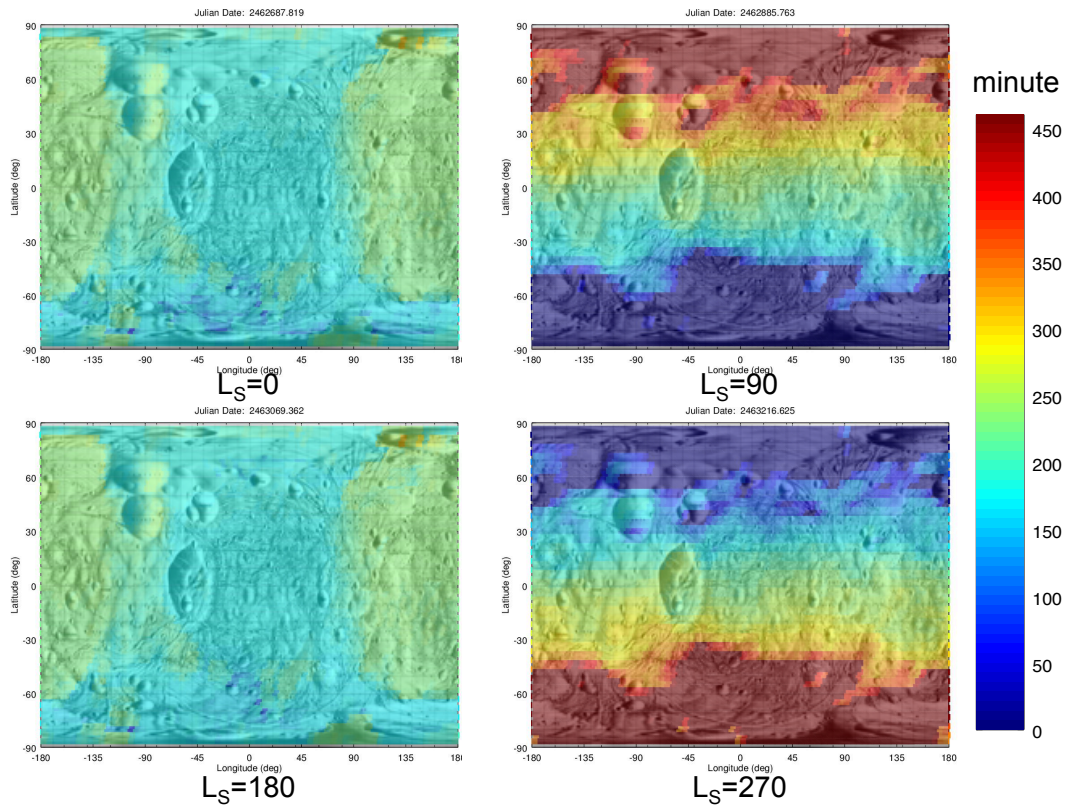


Figure 6. Surface exposure time per Phobos' orbit at equinoxes and solstices

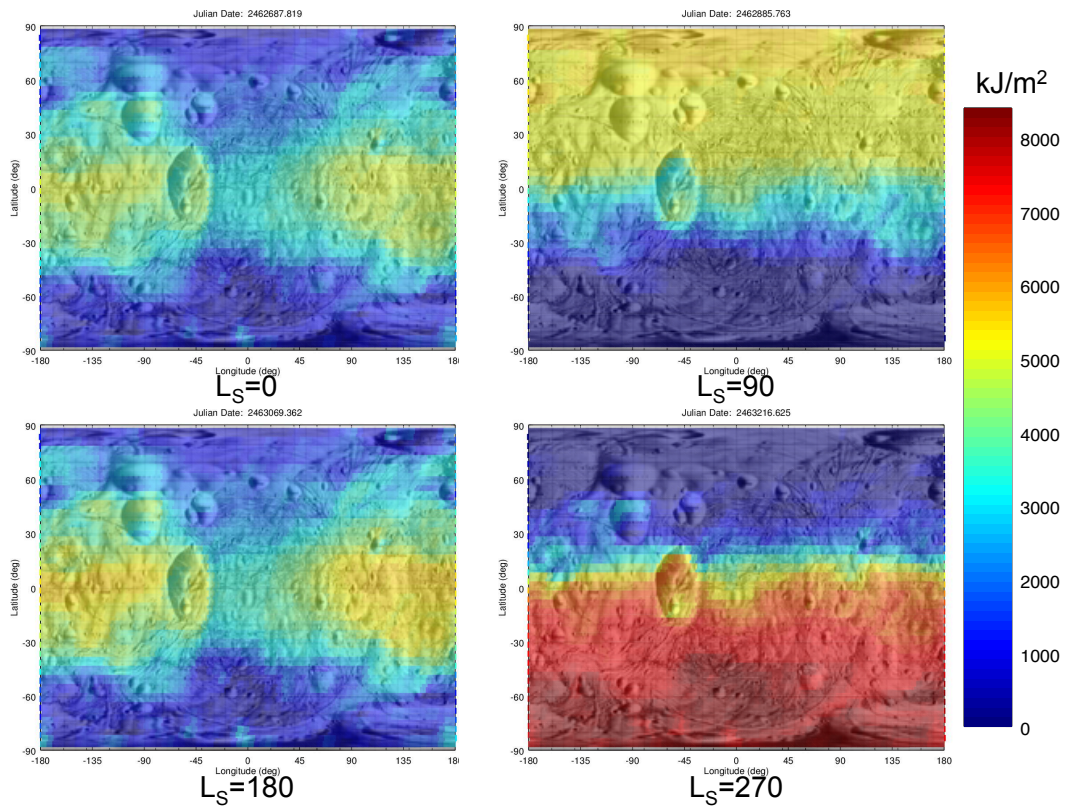


Figure 7. Radiant exposure over one Phobos' orbit for fixed solar array at equinoxes and solstices

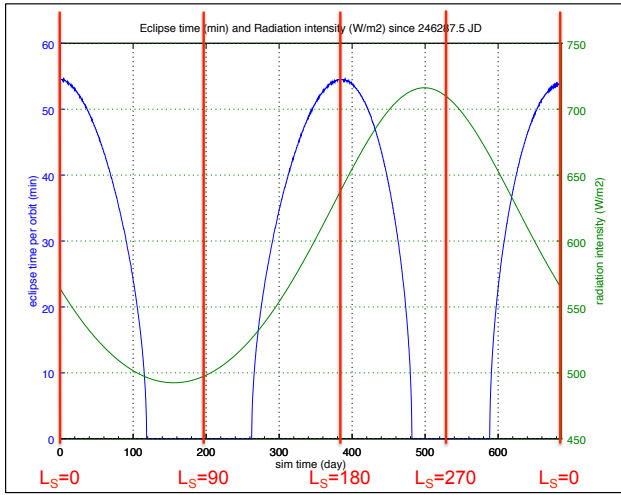


Figure 5. Radiation intensity and solar eclipse of Phobos

Radiant Exposure for Tracking Solar Array—represents the best scenario for energy generation. It assumed the solar array is able to track the motion of the sun perfectly such that the normal direction of the solar array is parallel to the sun vector. The result accounts for effects of solar radiation intensity and exposure time. Figure 8 shows four instances of the sun tracking array radiant exposure over one Phobos orbit at equinoxes and solstices.

4. USAGE EXAMPLE

This section presents a use case demonstrating the usefulness of these results in terms of mission analysis and vehicle design. The data is generated using a 450,000 facet STL Phobos model.

Lighting Condition at 11 Science Sites

Eleven preliminary sites were selected for their scientific exploration value, and Table 2 lists the longitude and latitude coordinate of these sites[8].

Figure 9 to Figure 11 present the lighting conditions at these 11 sites as function of time.

As expected, exposure time for sites near the equator is relatively constant over time compared to the exposure time for sites further from the equator. Exposure time for sites 5, 6, 9, 10, and 11 vary significantly with Martian seasons. Results for radiant exposure for fixed array include the effects of exposure time, radiation intensity and incident angle. Even though exposure time is similar during summer and winter for sites near the equator, radiation intensity is not. The difference in radiant exposure is significant between summer and winter. Compared to the fixed array, a sun tracking array could generate more energy per unit area, especially for sites in the northern hemisphere such as sites 5, 6, 9, and 10 during the winter.

Preliminary Power Subsystem Design Tool

Making use of the lighting condition results generated for the 11 science sites, a preliminary power subsystem analysis tool for a Phobos habitation lander was developed. The tool can generate battery and solar array sizing information based on the power load and solar array efficiency inputs.

Equations are presented in the Appendix. Input parameters for an example analysis are in Table 3.

Table 3. Example parameters for a habitation lander

Attributes	Value	Unit
Solar array total efficiency	20	%
Solar array type	sun tracking	–
Power load	10.0	kW
Battery max discharge %	80	%

Figure 12 shows the minimum surface area of the solar array needed for the lander as a function of time, and Figure 13 shows the minimum battery capacity needed for the lander as function of time, considering the desired maximum discharge percentage.

These results provide preliminary information for engineers in designing the power subsystem of the habitation lander operating at the 11 science sites.

5. CONCLUSION

A human mission to Phobos is one of several precursor missions under consideration to prepare the next giant leap on Mars. Among other environmental factors, lighting conditions play a crucial role for mission success. This study used a high fidelity computer simulation to investigate the lighting conditions on Phobos. The simulation includes an environment model, a Phobos model, and an occultation model. These models work together to provide reliable results of the lighting conditions on Phobos. The results show that the lighting condition changes significantly from one Martian season to another: radiation intensity changes from its minimum in late northern spring to its maximum in late fall; solar eclipse length is long during the spring and fall, and no solar eclipse occurs during the summer and winter; exposure time per orbit is relatively uniform over the surface during the spring and fall but varies with latitude during the summer and winter; a sun tracking solar array could generate 50 to 75 % more energy than a fixed solar array. It is hoped that these results will be useful in the vehicle design process for a future mission to Phobos.

APPENDIX

Radiation intensity

$$I_{Phobos} = I_{1AU} \frac{1}{d_{Phobos}^2} \quad (1)$$

Where I_{Phobos} is the solar radiation intensity (in unit of W/m^2) at Phobos, I_{1AU} ($\approx 1367 W/m^2$) is the solar radiation intensity of 1 Astronomical Unit (AU), and d_{Phobos} is the distance of Phobos with respect to the Sun in AU.

Radiation flux

$$\Phi = I_{Phobos} \cos(\theta) \delta_{expose} \quad (2)$$

Φ is the radiation flux (in unit of W/m^2) for a specific facet. θ is the angle between the Sun vector and a facet's

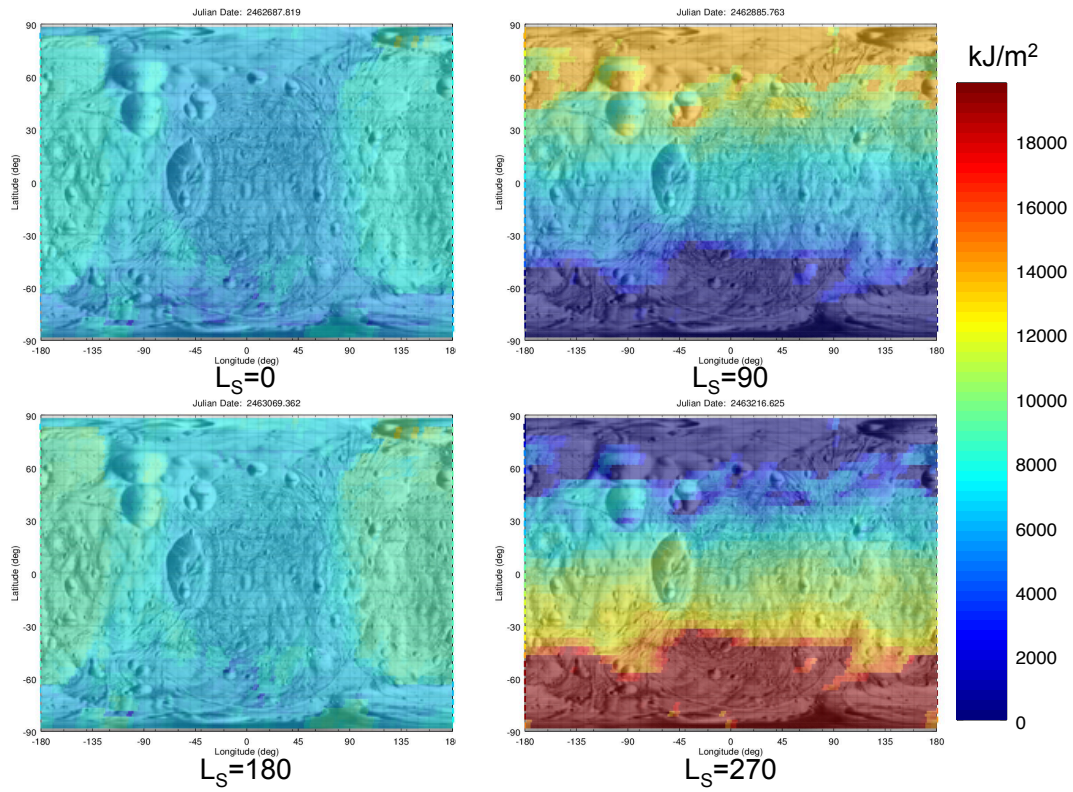


Figure 8. Radiant exposure over one Phobos' orbit for sun tracking solar array at equinoxes and solstices

Table 2. Coordinate of 11 science sites on Phobos

Site Num	1	2	3	4	5	6	7	8	9	10	11
Lat (deg)	-2	15	5	10	25	15	-5	-5	20	35	-25
Lon (deg)	-50	-45	-50	-35	-35	-20	-32	0	55	65	-15

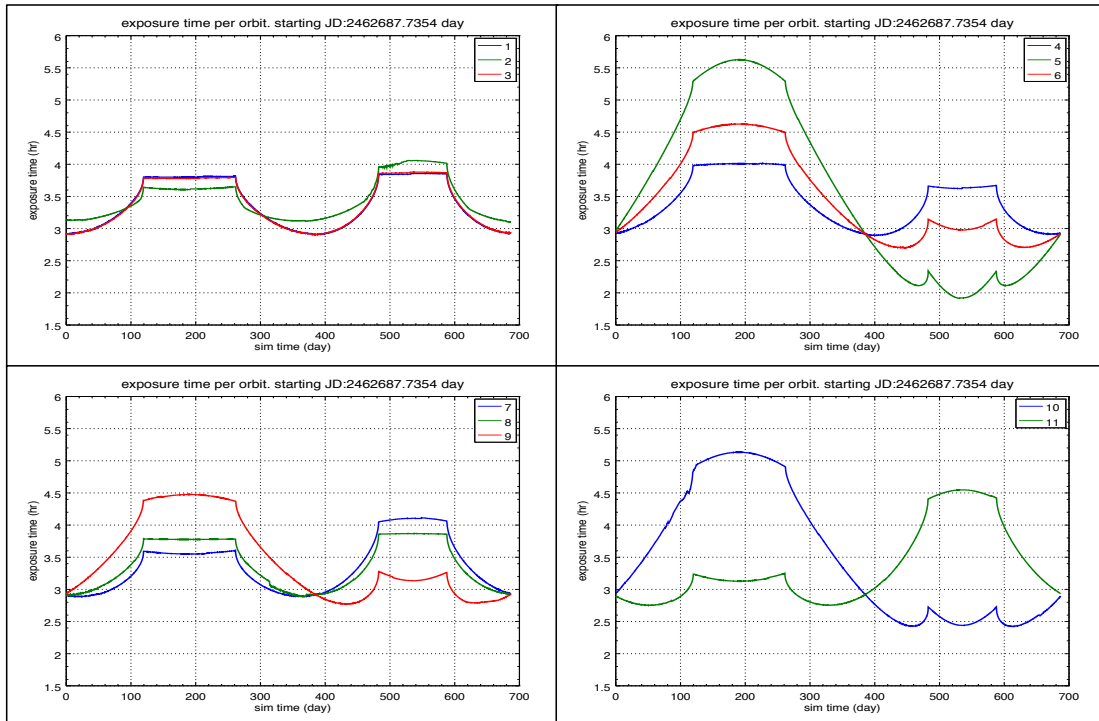


Figure 9. Surface exposure time per Phobos' orbit for site 1 to 11 (hr)

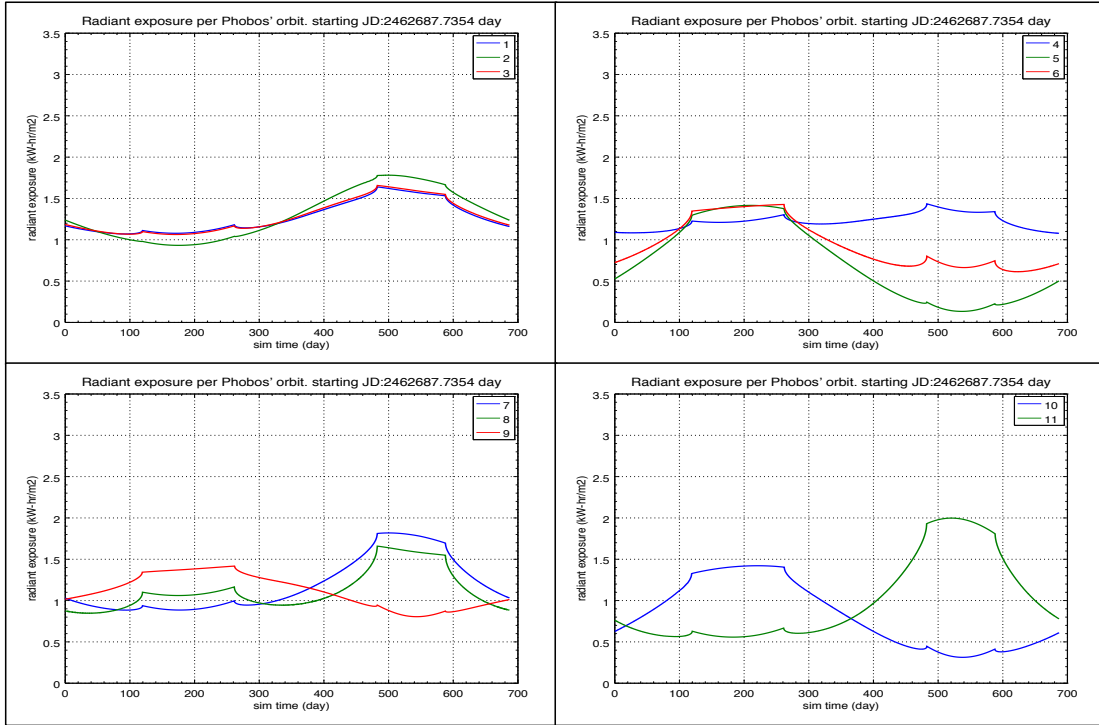


Figure 10. Radiant exposure per Phobos' orbit for a fixed array for site 1 to 11 ($kW \cdot hr/m^2$)

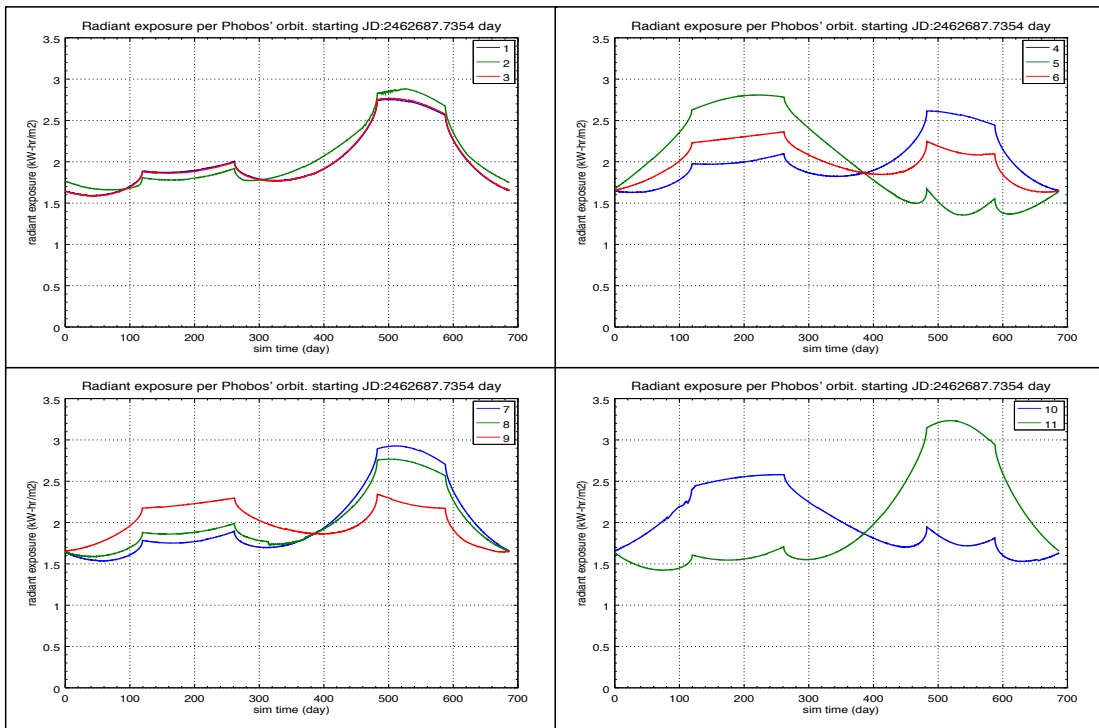


Figure 11. Radiant exposure per Phobos' orbit for a sun tracking array for site 1 to 11 ($kW \cdot hr/m^2$)

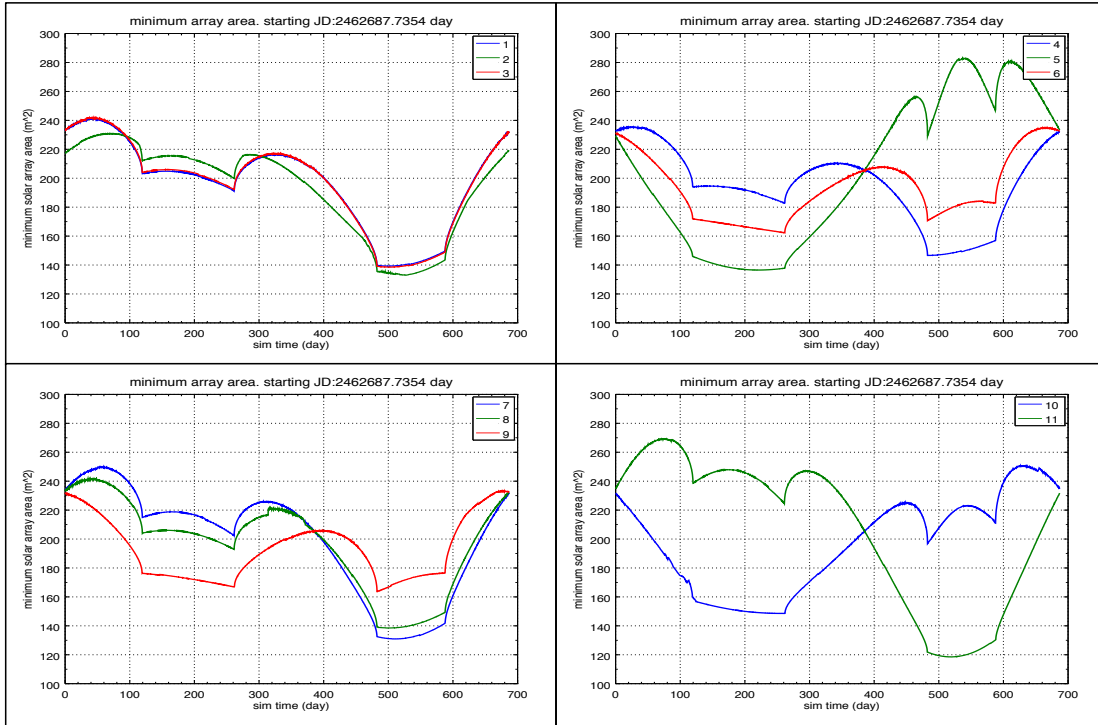


Figure 12. Minimum sun tracking solar array area for habitation lander (m^2)

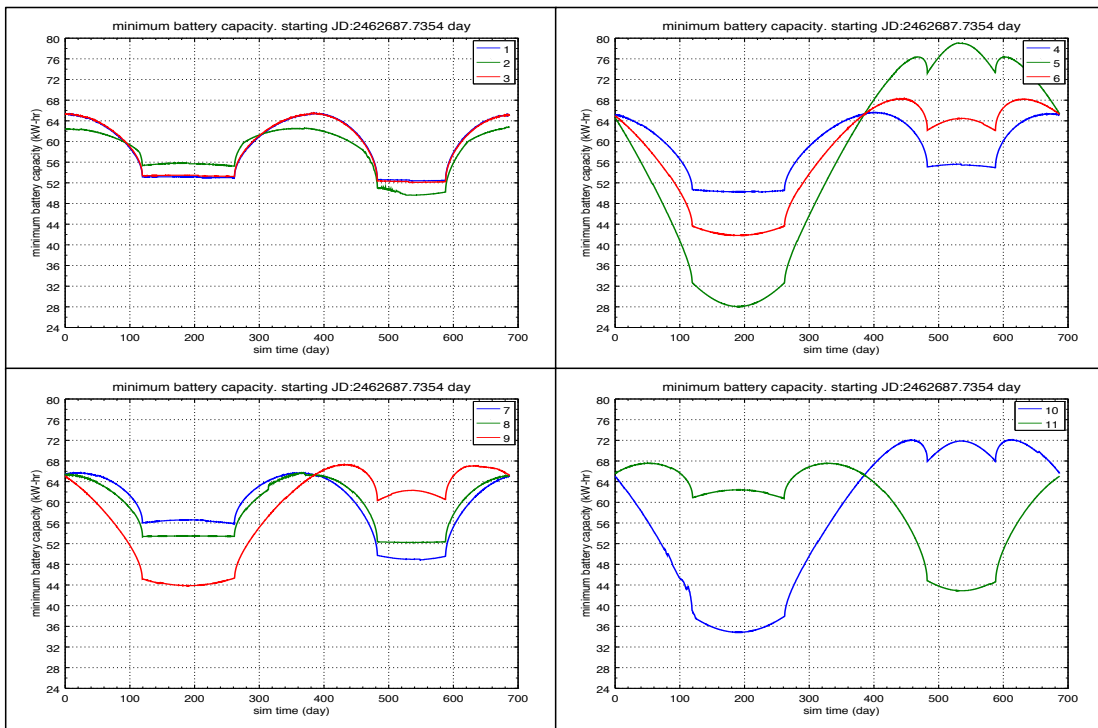


Figure 13. Minimum battery capacity needed for habitation lander ($kW \cdot hr$)

normal vector. δ_{expose} is the Kronecker delta function, which equals one when the facet is exposed to sun lighting or zero otherwise.

Minimum array area

$$A_{array} = \frac{t_{shadowed} P_{avg}}{\eta H_e} \quad (3)$$

Where A_{array} is the solar array area, $t_{shadowed}$ is the amount of time that the facet is in shadow for one Phobos' orbit, P_{avg} is the average power load for the vehicle, η is the solar array total efficiency, and H_e is the radiant exposure over one Phobos' orbit.

Minimum battery

$$C_{battery} = \frac{1.1 t_{shadowed} P_{avg}}{MD} \quad (4)$$

Where $C_{battery}$ is the battery capacity, MD is maximum discharge factor, and the constant coefficient is a correction factor to accommodate the additional energy that may be needed when power generation is smaller than the power load (consuming battery energy).

ACKNOWLEDGMENTS

The authors would like to thank everyone on the NASA's Exploration Systems Simulations (NExSyS) team for their constant support throughout the simulation development. Additionally, Zu Qun would like to thank Zack Crues, Dan Dexter, and Paul Bielski for their help and guidance throughout this study.

REFERENCES

- [1] G. A. Landis, "Footsteps to mars: An incremental approach to mars exploration," *Journal of the British Interplanetary Society*, vol. 48, pp. 367–342, 1995.
- [2] P. Lee, S. Braham, M. Silver, P. Thomas, and M. West, "Phobos: a critical link between moon and mars exploration," *Space Resources Roundtable VII*, 2005.
- [3] P. Lee, "Phobos-deimos asap: a case for the human exploration of the moons of mars," *Workshop on the Exploration of Phobos and Deimos*, 2007.
- [4] S. L. Murchie, D. T. Britt, and C. M. Pieters, "The value of phobos sample return," *Planetary and Space Science*, pp. 176–182, April 2014.
- [5] E. M. Standish, "Jpl planetary and lunar ephemerides, de405/le405," *JPL IOM*, no. 312.F - 98 - 048, August 1998.
- [6] (2015). [Online]. Available: <http://www.planetary.org/explore/space-topics/mars/mars-calendar.html>
- [7] [Online]. Available: <http://planetarynames.wr.usgs.gov/images/phobos-cylindrical-grid.pdf>
- [8] A. Abercromby, M. Gernhardt, S. Chappell, D. Lee, and A. Howe, "Human exploration of phobos," in *Aerospace Conference, 2015 IEEE*, March 2015, pp. 1–17.

BIOGRAPHY



Zu Qun Li received his B.S degree in aerospace engineering from the Pennsylvania State University in 2012 and a M.S degree in aerospace engineering in 2014. He is currently working in the Simulation and Graphics branch at NASA Johnson Space Center in Houston, Texas. He is also a member of NASA's Exploration Systems Simulation (NExSyS) team working on simulation development and analysis for future human space mission beyond lower Earth orbit.



Guy De Carufel Guy de Carufel works for Odyssey Space Research LLC in Houston Texas. He has a M.S degree in aerospace engineering, a B.S in mechanical engineering and completed the ISU Space Studies Program in 2009. His expertise includes space hardware and systems modeling, and flight software development such as the NASA Core Flight Software architecture. He also developed testing, integration and assembly procedures for several nanosatellites during his graduate degree.



Edwin Z. Crues Edwin Zack Crues has over 25 years of professional experience in developing spacecraft simulation and simulation technologies. Zack is currently a member of the Simulation and Graphics branch at NASAs Johnson Space Center in Houston, Texas (<http://er.jsc.nasa.gov/ER7>) where he leads the development of simulation technologies and the application of those technologies in the simulation of NASAs current and proposed crewed spacecraft. He has developed hundreds of models and simulations for NASA spacecraft including Shuttle, International Space Station (ISS), Orion, Altair, Morpheus and the Multi-Mission Space Exploration Vehicle. Zacks recent research focus has been developing and applying distributed computation and distributed simulation technologies. This includes a large-scale distributed simulation of NASAs proposed human space exploration missions. Zack also has international experience in developing simulations of European Space Agency launch systems and Japanese Aerospace Exploration Agency spacecraft.



Paul Bielski Paul Bielski is the lead of the NASA Exploration Systems Simulation (NExSyS) team at NASA's Johnson Space Center. After obtaining a B.S. in aerospace engineering from the University of Notre Dame in 1989, he developed spacecraft flight and ground systems for government and commercial entities, worked with international partners to advance on-orbit and ground-based robotic systems, and applied modeling and simulation technology to support analysis, development, test, and operation of existing and future NASA spacecraft.